MOLECULAR ECOLOGY

Molecular Ecology (2017) **26**, 457–470 doi: 10.1111/mec.13932

Recombination rate variation in mice from an isolated island

RICHARD J. WANG,* MELISSA M. GRAY,* MICHELLE D. PARMENTER,* KARL W. BROMAN† and BRET A. PAYSEUR*

*Laboratory of Genetics, University of Wisconsin – Madison, 425-G Henry Mall, 2428 Genetics, Madison, WI 53706, USA, †Department of Biostatistics & Medical Informatics, University of Wisconsin – Madison, Madison, WI 53706, USA

Abstract

Recombination rate is a heritable trait that varies among individuals. Despite the major impact of recombination rate on patterns of genetic diversity and the efficacy of selection, natural variation in this phenotype remains poorly characterized. We present a comparison of genetic maps, sampling 1212 meioses, from a unique population of wild house mice (*Mus musculus domesticus*) that recently colonized remote Gough Island. Crosses to a mainland reference strain (WSB/EiJ) reveal pervasive variation in recombination rate among Gough Island mice, including subchromosomal intervals spanning up to 28% of the genome. In spite of this high level of polymorphism, the genomewide recombination rate does not significantly vary. In general, we find that recombination rate varies more when measured in smaller genomic intervals. Using the current standard genetic map of the laboratory mouse to polarize intervals with divergent recombination rates, we infer that the majority of evolutionary change occurred in one of the two tested lines of Gough Island mice. Our results confirm that natural populations harbour a high level of recombination rate polymorphism and highlight the disparities in recombination rate evolution across genomic scales.

Keywords: island evolution, linkage map, recombination, recombination rate evolution

Received 16 August 2016; revision received 9 November 2016; accepted 14 November 2016

Introduction

Recombination ensures the fidelity of chromosome pairing and segregation during meiosis (Tsubouchi & Roeder 2003; Hassold *et al.* 2007; Lao *et al.* 2013). Recombination also shapes evolution by shuffling alleles across genetic backgrounds, increasing the efficacy of selection and muddling a population's genealogical history (Felsenstein 1974; Otto & Lenormand 2002; Griffiths & Marjoram 1996; Schierup & Hein 2000). Despite recombination's conserved functional roles, its rate varies among individuals, within and between species (True *et al.* 1996; Graffelman *et al.* 2007; Coop *et al.* 2008; Dumont & Payseur 2011a; Smukowski & Noor 2011; Comeron *et al.* 2012). Recombination rate shows resemblance among relatives (Kong *et al.* 2004; Coop *et al.* 2008; Fledel-Alon *et al.* 2011), maintains strain differences in a common environment (Koehler *et al.* 2002; Dumont & Payseur 2011b; Baier *et al.* 2014) and responds to artificial selection (Chinnici 1971; Kidwell & Kidwell 1976; Charlesworth & Charlesworth 1985), revealing a genetic component to individual variation. Multiple loci, including specific genes, that confer recombination rate differences have been identified (Kong *et al.* 2008; Murdoch *et al.* 2010; Dumont & Payseur 2011b; Parvanov *et al.* 2010; Sandor *et al.* 2012; Ma *et al.* 2015; Johnston *et al.* 2016; Hunter *et al.* 2016).

Patterns of individual variation in recombination rate depend on the genomic scale of measurement. Cytological techniques, which visualize and enumerate crossovers in meiocytes (Anderson *et al.* 1999; Koehler *et al.* 2002; Baier *et al.* 2014), offer direct estimates of the genomewide recombination rate. At this scale, individual recombination rates are constrained by the requirement that each chromosome (or chromosome arm) has at least one crossover for proper chromosome segregation (Mather 1936; de Villena & Sapienza 2001; Fledel-Alon

Correspondence: Bret A. Payseur, Tel: (608) 890-0867, Fax: (608) 262-2976; E-mail: payseur@wisc.edu

et al. 2009). The connection between recombination rate and karyotype is perhaps most visible in the elevated recombination rates of bird species with genomes that are rich in microchromosomes (Burt 2002; Groenen *et al.* 2009; Backstrom *et al.* 2010). Beyond this karyotypic pattern, the genomewide recombination rate shows a phylogenetic signal across mammals (Dumont & Payseur 2008; Segura *et al.* 2013; Froehlich *et al.* 2015), suggesting that evolution proceeds at a slow to moderate pace.

Genetic linkage maps reveal heterogeneity in recombination rate on the chromosomal scale. Along a chromosome, recombination is often suppressed near the centromere and elevated in distal regions (Beadle 1932; Mahtani & Willard 1998; Lynn *et al.* 2004; Talbert & Henikoff 2010). Sex appears to be a major determinant of these stereotypical patterns: elevated recombination near telomeres predominates in males from a variety of species (Broman *et al.* 1998; Kochakpour & Moens 2008; Giraut *et al.* 2011; Liu *et al.* 2014; Ma *et al.* 2015; Smeds *et al.* 2016). Several genomic parameters correlate with recombination rate across the genome, including gene density, GC content, nucleotide diversity, repetitive elements, chromosome position and certain sequence motifs (Begun & Aquadro 1992; Eyre-Walker 1993; Fullerton *et al.* 2001; Rizzon *et al.* 2002; Kong *et al.* 2002; Jensen-Seaman *et al.* 2004; Winckler *et al.* 2005; de Massy 2013). A subset of megabase-sized intervals also exhibit significant differences in recombination rate among individuals (Broman *et al.* 1998; Kong *et al.* 2002; Dumont *et al.* 2011; Smukowski & Noor 2011; Comeron *et al.* 2012).

On the finer scale, recombination rates across the genome can span orders of magnitude. In humans, mice, and yeast, crossovers are concentrated in kilobase-sized regions termed 'recombination hotspots' (Gerton *et al.* 2000; Jeffreys *et al.* 2001; Paigen *et al.* 2008). Sperm genotyping demonstrates variation in the intensity and position of recombination hotspots among men (Cullen *et al.* 2002; Neumann & Jeffreys 2006; Tiemann-Boege *et al.* 2006; Webb *et al.* 2008). Comparisons of linkage disequilibrium suggest rapid evolution of hotspots among human populations (McVean *et al.* 2004; Evans & Cardon 2005) and other primates (Ptak *et al.* 2005; Winckler *et al.* 2005; Brunschwig *et al.* 2012), but evolutionary stasis among finches (Singhal *et al.* 2015).

The collection of techniques for quantifying recombination rate currently forms a disjointed picture of how recombination evolves. Estimating recombination rate from the transmission of markers among relatives offers key advantages for characterizing recombination rate evolution. In contrast to other approaches, genetic linkage maps measure current recombination rates across the entire genome and traverse the many genomic scales on which recombination rate varies. High-resolution genetic maps exist for a growing number of species (Kong *et al.* 2002; Cox *et al.* 2009; Rockman & Kruglyak 2009; Comeron *et al.* 2012; Kawakami *et al.* 2014). Despite this progress, statistical comparisons among genetic maps with the purpose of quantifying recombination rate evolution remain rare (Poissant *et al.* 2010; Dumont *et al.* 2011; Comeron *et al.* 2012; Ross *et al.* 2015). Genomic scans for specific intervals that show heritable variation in recombination rate among individuals from a single natural population are even less common (but see Comeron *et al.* 2012).

Recombination has been studied more extensively in laboratory mice (*Mus musculus*) than in any other vertebrate, combining dense genetic maps (Shifman *et al.* 2006; Cox *et al.* 2009; Liu *et al.* 2014) with mechanistic studies (Holloway *et al.* 2008; Paigen & Petkov 2010; Bolcun-Filas & Schimenti 2012; Cole *et al.* 2014; Hunter *et al.* 2016). This work provides a rich context for understanding the evolution of recombination in wild mice. At the same time, distinct histories and environments raise the prospect that recombination experiences contrasting evolutionary dynamics in wild mice and laboratory mice. Although studies of human pedigrees have detected individual differences in recombination rate (Broman *et al.* 1998; Kong *et al.* 2002), mice provide additional advantages as a model system. First, genetic and nongenetic contributions to recombination rate can be separated—a challenging task in humans—by raising mice in a common environment. This possibility is important in light of the evidence that recombination rate is shaped by an array of environmental factors (Bomblies *et al.* 2015). Second, inbred mice can be used to generate large recombinant families, providing statistical power to identify recombination rate differences among strains in subchromosomal intervals.

Here, we take advantage of an unusual population of wild mice to understand how recombination rate evolves in nature. Gough Island is a remote, South Atlantic island that was colonized by house mice, probably only a few hundred generations ago (Gray *et al.* 2014). By comparing genetic maps, we find substantial variation in the recombination rate on multiple genomic scales between two lineages of mice from this isolated island. In contrast to most previous examinations of recombination rate variation, we identify specific genomic intervals with heritable differences in rate within a single natural population.

Materials and methods

Mice, crosses and genotyping

Intercrosses involved mice derived from Gough Island and the wild-derived inbred strain WSB/EiJ (Jackson

Laboratory, Bar Harbor, ME), which is descended from mainland North America. Gough Island is a remote volcanic island in the South Atlantic Ocean, part of a protected wildlife refuge that has been designated a UNESCO World Heritage Site. Mice from Gough Island (GI) were live-trapped and transported to the Charmany Instructional Facility at the University of Wisconsin—Madison. A breeding colony consisting of 25 mature females and 21 mature males was established. All mice were housed in microisolator cages separated by sex in a temperature-controlled room (68°–72°F) set to a 12-h light/dark cycle. Food (Teklad 6% fat mouse/rat diet; Harlan Laboratories, Madison, WI) and water were provided *ad libitum*, corn cobs ground to one-eighth inch were provided for bedding (Waldschmidt and Sons, Madison, WI), and irradiated sunflower seeds (Harlan Laboratories) and nesting material were provided weekly for enrichment. For identification, pups were toe-tattooed with sterile lancets and tattoo paste starting at 1 week, while ears were punched at weaning (3–4 weeks) to identify adults. Additional details on the transport, housing and establishment of the breeding colony of GI mice can be found in Gray *et al.* (2015).

We began the intercrosses with a full-sib male and female chosen from each of two partially inbred lines in our breeding colony of GI mice, denoted as Line A and Line B. These lines were created from four generations of full-sib mating among the laboratory-born offspring of wild GI mice. The four mice, one male and one female from each of Line A and Line B, were each crossed with WSB/EiJ to generate four independent sets of F_1s and four F_2 intercrosses (Fig. 1). We generated 497 F_2 mice from the Line A cross and 877 F_2s mice from the Line B cross, for a total of 1374 F_2s. Among these mice, 419 from the Line A cross and 793 from the Line B cross were incorporated into subsequent analyses after removing mice that were not genotyped or contained obvious genotyping errors.

Mice were genotyped on the Mega Mouse Universal Genotyping Array (MEGAMUGA; Morgan *et al.* 2016), an Illumina Infinium array containing 77 808 markers. The vast majority of markers on the array are single

Fig. 1 Cross design. Partially inbred lines of Gough Island mice were crossed with the wild-derived inbred strain WSB/EiJ. Four independent F_2 intercrosses were generated from these crosses.

nucleotide polymorphisms (SNPs), although a few structural and transgenic markers are also present. Markers cover the autosomes, sex chromosomes and mitochondria with an average spacing of ~33 kb across the genome. Liver tissue from F_2 individuals, as well as controls, was sent to GeneSeek (NeoGene, Lincoln, Nebraska) for DNA extraction and genotyping. Samples were divided among 16 96-well plates, and several steps were taken to identify and control for errors. WSB samples were placed on each plate to account for plate extraction effects, parental GI samples were replicated across plates, and the sample from the first well of each plate was replicated across plates. Markers with high rates of missing data were omitted, as were mice with high rates of missing genotypes. We removed a small number of individuals that showed many Mendelian inconsistencies or mismatched genotypic and phenotypic sex.

Construction and comparison of genetic maps

To construct and compare genetic maps, we selected a subset of 11 833 informative SNPs from our genotype data. These SNPs were invariant among the GI mice we genotyped and displayed the segregation patterns expected for a standard F_2 intercross between inbred lines. Distances between informative markers and the total number of crossovers recorded for each chromosome are summarized in Table S2 (Supporting information). Mapping distances for each cross were estimated from these SNPs using the Lander–Green hidden Markov model (Lander & Green 1987) implemented in the R/qtl est.map function (Broman & Sen 2009). We assumed a genotyping error rate of 0.2% and converted recombination fractions to map distances with the Carter–Falconer map function (Carter & Falconer 1951). To determine thresholds for statistical significance in map length comparisons, we permuted line labels across mice and reconstructed genetic maps. We performed 2000 permutations, retaining the numbers of mice labelled as Line A or Line B in each permutation. The map length of a chromosome was determined to be significantly different between GI lines if the observed difference was at least as extreme as 5% of differences for that chromosome among permutations. We used the same approach to test for significant differences in overall map length.

To compare recombination rates among GI lines on a finer scale, we examined map lengths in sliding windows across the genome. Windows spanned 10, 25 and 50 Mb with a step size of 250 kb. We calculated a *P*-value for the observed difference in map length of each window as the proportion of replicates that produced a difference greater than or equal to the observed value. Each window had a respective set of 2000 permutations from which we calculated the *P*-value. To

control for false positives arising from multiple testing in these overlapping windows, we used a false discovery rate approach (Storey & Tibshirani 2003). We calculated a q-value for each window using the full set of P-values across all windows and rejected the null hypothesis of no difference in map length at $q < 0.1$. The distributions of P-values across windows were not independent, but our use of an empirical null should be conservative (Leek & Storey 2011). We combined overlapping windows showing significant differences to generate a final list of divergent intervals. We checked the performance of the multiple testing correction by looking for windows with significantly different map lengths in an additional set of 100 permuted maps. After controlling for false discovery using our larger set of 2000 permutations, each set of 100 permuted maps had an average of less than 10 significant windows at the $q < 0.1$ level. This is the number of significant windows we should expect in the absence of true differences in recombination rate. Finally, it is possible that the difference in sample size between the two GI line crosses could contribute to observed variation in recombination rate. To account for this effect, we repeated the search for significantly different windows with an equivalent number of mice from the two lines. Specifically, we randomly selected a subset of 419 F_2 individuals from Line B to match the number in Line A, constructed maps from this subset and created 1000 sets of permuted maps from this subset to calculate P-values.

To provide perspective for the differences in recombination rate between GI lines, we conducted additional comparisons with the mouse reference genetic map (downloaded from http://cgd.jax.org/mousemapconverter/). The mouse reference genetic map features data from a heterogeneous stock (HS) mouse population derived from crosses involving eight classically inbred strains (Shifman *et al.* 2006; Cox *et al.* 2009). The HS map, which sampled 3546 meioses, was constructed from genotypes at 10 195 SNPs. For comparison to GI maps, we converted the HS map positions from the Kosambi map function to the Carter–Falconer map function and anchored the proximal markers of the GI maps using interpolated recombination rates, following the practice in Cox *et al.* (2009). We re-estimated recombination rates for the HS map in sliding windows using the approach as described above. We computed correlations in recombination rate by comparing the same windows in the HS and GI maps.

Genomic features, sequencing and motif search

To identify potential determinants of recombination rate variation, we calculated correlations between genomic features known to be associated with recombination and differences in recombination rate among GI lines. Positions of genomic features were downloaded from the UCSC annotation database for NCBI Build 37/mm9. For chromatin state, annotations by CHROMHMM (Ernst & Kellis 2012) on mouse testis—the only annotated germline tissue—were downloaded from the Mouse ENCODE Consortium (2012; Yue *et al.* 2014). To evaluate the influence of evolutionary breakpoint regions (Farré *et al.* 2013; Ullastres *et al.* 2014), we identified 364 such regions in a synteny analysis between the mouse and human reference genomes with CASSIS (Lemaitre *et al.* 2008; Baudet *et al.* 2010).

To minimize autocorrelation, we estimated recombination rate in nonoverlapping windows for these analyses, again sized at 10, 25 and 50 Mb. We also compared recombination rate differences among GI lines to rates estimated in corresponding nonoverlapping windows for the HS map.

The PRDM9 protein is a major determinant of crossover position in the mouse genome (Baudat *et al.* 2010; Parvanov *et al.* 2010; Grey *et al.* 2011). We used new genome sequences to test the prediction that windows with divergent recombination rates are enriched for polymorphic binding sites for PRDM9. We sequenced the genomes of the four GI parents of our intercrosses at an average 10× coverage using 100-bp paired-end reads on an Illumina HiSeq 2500. Reads were mapped to the C57BL/6 mouse reference genome using the Burrows–Wheeler Aligner (Li & Durbin 2009) and SNPs were called with SAMTOOLS 1.0 (Li *et al.* 2009). Using these sequences, we identified fixed differences between GI lines A and B and constructed a 50-bp window centred on each fixed difference. We used this set of windows to query against the consensus PRDM9 binding motif using its position weight matrix (Brick *et al.* 2012) and FIMO from the MEME Suite of bioinformatics tools (Grant *et al.* 2011). Additionally, we performed a signed test in intervals with divergent recombination rates to determine whether the number of variable motifs correlated with the direction of divergence. Finally, we used PCR primers fl1500U20, mZPrdm9-R1, Meis284L23 and mZPrdm9-F1 (Buard *et al.* 2014) to amplify the last exon of PRDM9 in the GI lines. We ran the PCR products on 1% agarose gels to determine whether their sizes matched alleles known to confer recombination rate differences within *M. m. domesticus* (Buard *et al.* 2014).

Results

We documented recombination rate variation between two lines of Gough Island (GI) mice (Line A and Line B) by comparing genetic maps built from two sets of F_2 intercrosses with a common reference strain (WSB/EiJ).

The genomewide recombination rate, represented by total map length, was similar, at 1340 cM (Line A) and 1347 cM (Line B). Despite similarity in the genomewide rate, five chromosomes (2, 5, 8, 9 and 18) showed statistically significant differences in map length (Table 1). Notably, chromosome 8 was 16% longer in Line B. This disparity among five chromosomes represents a significant departure from the expectation that no difference exists between the two GI lines ($P < 0.002$; Fisher's combined P-value test).

To measure variation in recombination rate on a subchromosomal scale, we tiled the genome with overlapping windows of fixed physical size and compared map lengths across pairs of corresponding windows for the two lines. We repeated the analysis with three window sizes—50, 25 and 10 Mb—to capture differences in recombination rate on multiple scales. We found 500 (50-Mb windows), 483 (25 Mb) and 165 (10 Mb) windows with significant recombination rate differences. These numbers exceed null expectations generated by analyses of permuted data sets (see Methods). On all three scales, windows that exhibited significantly different map lengths were typically adjacent to other significant windows (Fig. 2). We combined significant windows that overlapped into discrete intervals for further analysis. Fourteen chromosomes harboured intervals with divergent recombination rate on at least one scale (Table 2); these intervals often displayed divergence across multiple window sizes (Fig. 2). It is notable that no divergent intervals were identified on the X chromosome. Similar comparisons of recombination rate made between strains from different subspecies (*Mus musculus castaneus* and *Mus musculus musculus*) identified a disproportionately large number of divergent intervals on the X chromosome (Dumont *et al.* 2011).

Table 1 Genetic map lengths for each chromosome in two lines of Gough Island mice

Chr	Line A (cM)	Line B (cM)	Diff. (cM)	% diff.	P-value
1	94.35	92.01	2.34	2.5	0.444
2	89.18	96.15	−6.97	−7.5	0.019*
3	72.90	73.39	−0.49	−0.7	0.897
4	76.83	76.40	0.43	0.6	0.852
5	77.88	84.09	−6.21	−7.7	0.041*
6	70.61	69.21	1.40	2.0	0.627
7	75.89	78.64	−2.75	−3.6	0.338
8	60.10	70.24	−10.14	−15.6	0.001*
9	59.85	65.24	−5.39	−8.6	0.032*
10	67.17	67.73	−0.56	−0.8	0.839
11	81.01	76.22	4.79	6.1	0.092
12	58.00	57.27	0.73	1.3	0.744
13	55.21	56.25	−1.04	−1.9	0.675
14	60.29	57.96	2.33	3.9	0.340
15	52.18	54.82	−2.64	−4.9	0.291
16	54.22	52.83	1.39	2.6	0.509
17	55.12	53.17	1.95	3.6	0.427
18	56.52	50.59	5.93	11.1	0.006*
19	51.99	49.39	2.60	5.1	0.231
X	70.25	65.64	4.60	6.8	0.221
Total	1339.55	1347.24	−7.69	−0.6	0.562

Asterisks highlight chromosomes with significantly different map lengths at the $P < 0.05$ level. P-values are calculated from two-tailed tests using 2000 permutations. Per cent difference calculated as ($Length_{LineA}$–$Length_{LineB}$)/Mean.

The magnitude of variation in recombination rate was inversely correlated with interval size ($P < 5 \times 10^{-5}$). The greatest differences in recombination rate, as percentages of the mean (109% on chromosome 1) and as absolute differences (0.61 vs. 0.96 cM/Mb on chromosome 18), were visible in the 10-Mb window analysis. In many cases, intervals discovered while scanning with smaller windows localized differences found in scans with larger windows. For example, among the differences in map length found on chromosome 15, which were identified at all three scales, the majority localized to a single 12.5-Mb interval.

Patterns of variation in recombination rate from these subchromosomal intervals generally matched patterns at the chromosome and genome levels. Chromosomes with significantly different map lengths (Table 1) contained intervals with consistent differences. Total differences in map length, as a sum of the divergence in all intervals, were not statistically significant on any window size—mirroring the absence of a significant difference in the whole-genome recombination rate. These observations suggest that coarse variation in recombination rate is due to the clustering of differences at finer scales. Chromosomes 8 and 9 showed a contrasting pattern: most of the differences in recombination rate on these chromosomes were only significant when surveyed at the 50 Mb or whole chromosome level. However, differences in statistical power are a challenge when comparing rates across chromosomes. Longer chromosomes have many fewer crossovers per Mb, reducing our ability to detect differences at finer scales.

Comparison to the standard mouse genetic map

Variation in the genetic maps described thus far represents an estimate of recombination rate polymorphism between two GI mice. To place this variation in a broader perspective, we compared the two genetic maps from crossing GI mice to WSB/EiJ with the standard genetic map of the laboratory mouse (the HS map). On the genomewide level, the GI maps, at 1388 cM (averaged and converted to match the HS analysis), were shorter than the 1457 cM of the HS map.

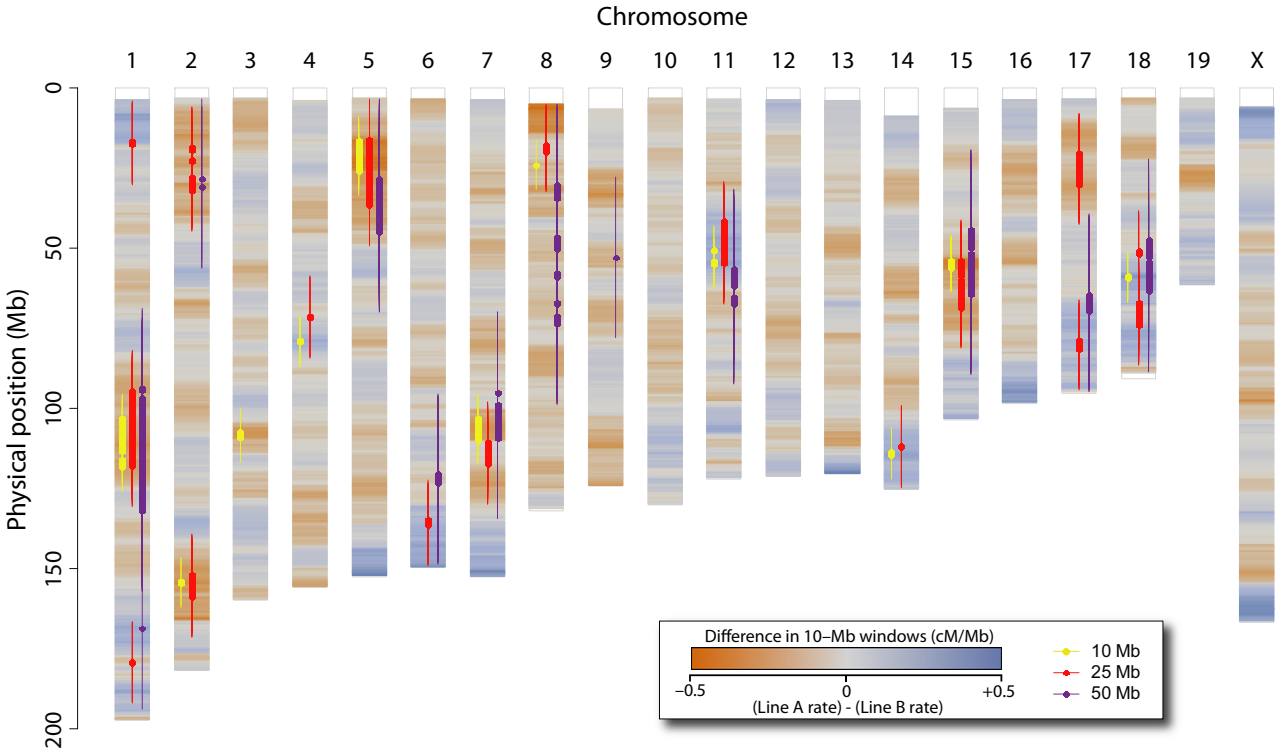

Fig. 2 Recombination rate differences between two lines of Gough Island Mice. Differences in recombination rate between two lines of Gough Island mice visualized as a gradient along chromosomes. Intensity of gradient from blue to orange indicates greater relative recombination rate in Line A and Line B, respectively. Plot markers with whiskers show centre and range of 10-, 25- and 50-Mb windows where recombination rates differ significantly (10% FDR). [Colour figure can be viewed at wileyonlinelibrary.com].

Local recombination rates in both GI lines were highly correlated with those in the HS (Table 3). Overall, the GI maps showed higher correlation with each other than with the HS map, with the degree of correlation decreasing as resolution increased.

We further investigated the relationship between the GI maps and HS map by focusing on windows for which recombination was significantly divergent between GI lines. Following the pattern observed in the comparison between GI lines, rate differences between the GI and HS maps were more pronounced in smaller windows (Table 2). By assuming that the two GI lines are more closely related to each other than either is to the collection of strains that comprise the HS (*i.e.* HS is the outgroup), we could polarize the changes in recombination rate in the GI lines. We observed a consistent bias: most GI-divergent intervals showed greater rate differences between Line A and the HS than between Line B and the HS (paired t-test, intervals from windows 50 Mb: $P = 0.093$, 25 Mb: $P = 0.004$, 10 Mb: $P = 0.037$) (Table 2). This bias was also seen in the collection of significantly different sliding windows, for which Line A rates showed substantially greater dispersion from HS rates (Levene's test, $P < 1 \times 10^{-15}$ for all three window sizes). Figure 3 illustrates this for 25-Mb windows; the greater squared residual deviation of rates from Line A relative to HS can be seen in the third panel. We repeated this analysis using a random subset of individuals from Line B, matching the number of individuals in Line A to account for the possibility that the smaller sample size in Line A was responsible for its higher divergence from HS. This power-matched comparison detected 71% as many significant windows as did the analysis with the full sample, but these significant windows continued to show higher dispersion from HS in Line A vs. Line B (Levene's test, $P < 5 \times 10^{-5}$ for all three window sizes). This pattern suggests that evolution in Line A was disproportionately responsible for differences between GI lines. For example, the 109% difference between GI lines in a region of chromosome 1 mostly reflects an evolutionary reduction in recombination rate in Line A.

Correlates of recombination rate polymorphism

Within-genome variation in recombination rate has been associated with a variety of genomic characteristics, including GC content, classes of repetitive elements, chromatin structure, gene density, evolutionary breakpoint regions and distance from the centromere

Table 2 Regions of divergent recombination between Gough Island lines

Physical position (Mb)				Line A rate	Line B rate		HS rate	% diff. with	
Chr	Begin	End	Size	(cM/Mb)	(cM/Mb)	% diff.	(cM/Mb)	Line A	Line B
50-Mb windows									
1	68.7	156.9	88.25	0.291	0.354	−20	0.365	−20	−3
1	143.7	193.7	50	0.717	0.617	15	0.692	4	−11
2	3.3	56.1	52.75	0.500	0.582	−15	0.563	−11	3
5	3.4	69.9	66.5	0.426	0.535	−23	0.527	−19	2
6	95.4	148.4	53	0.692	0.587	16	0.638	9	−8
7	69.9	134.4	64.5	0.408	0.502	−21	0.542	−25	−7
8	5.1	98.6	93.5	0.370	0.460	−22	0.493	−25	−7
9	27.8	77.8	50	0.480	0.574	−18	0.583	−18	−2
11	31.5	92.3	60.75	0.620	0.527	16	0.631	−2	−17
15	19.1	89.4	70.25	0.430	0.497	−14	0.523	−18	−5
17	39.3	94.6	55.25	0.814	0.711	14	0.754	8	−6
18	22.2	88.5	66.25	0.748	0.638	16	0.704	6	−9
					Total	0.8	**Total**	−2.9	−2.0
25-Mb windows									
1	3.9	30.2	26.3	0.603	0.456	28	0.370	63	23
1	81.9	130.4	48.5	0.179	0.291	−48	0.294	−39	−1
1	166.4	191.9	25.5	0.929	0.743	22	0.940	−1	−21
2	5.8	44.6	38.8	0.456	0.607	−28	0.611	−25	−1
2	139.1	171.3	32.3	0.557	0.732	−27	0.793	−30	−8
4	58.5	84.3	25.8	0.432	0.310	33	0.295	47	5
5	3.4	49.2	45.8	0.366	0.543	−39	0.532	−31	2
6	122.2	148.9	26.8	0.892	0.740	19	0.790	13	−6
7	97.9	129.9	32.0	0.294	0.406	−32	0.503	−42	−19
8	5.1	32.4	27.3	0.410	0.537	−27	0.594	−31	−10
11	29.0	67.3	38.3	0.718	0.599	18	0.645	11	−7
14	98.9	124.7	25.8	0.762	0.597	24	0.678	12	−12
15	41.1	81.1	40.0	0.408	0.554	−30	0.556	−27	0
17	7.8	42.6	34.8	0.251	0.365	−37	0.429	−41	−15
17	66.1	94.1	28.0	1.063	0.878	19	0.908	17	−3
18	38.2	64.5	26.3	0.708	0.543	26	0.661	7	−18
18	54.2	86.5	32.3	1.013	0.818	21	0.907	12	−10
					Total	0.1	**Total**	−1.8	−1.7
10-Mb windows									
1	97.9	123.2	25.3	0.064	0.218	−109	0.203	−68	7
2	148.8	159.6	10.8	0.259	0.487	−61	0.611	−58	−20
3	102.2	114.2	12.0	0.205	0.386	−61	0.356	−43	8
4	73.5	84.3	10.8	0.502	0.272	59	0.351	43	−23
5	11.2	30.9	19.8	0.336	0.606	−57	0.652	−48	−7
7	97.9	114.9	17.0	0.172	0.277	−47	0.370	−54	−25
8	18.9	28.9	10.0	0.203	0.395	−64	0.588	−65	−33
11	45.5	60.0	14.5	0.754	0.476	45	0.719	5	−34
14	108.4	119.4	11.0	0.686	0.385	56	0.568	21	−32
15	48.6	61.1	12.5	0.340	0.584	−53	0.571	−41	2
18	53.5	64.2	10.8	0.958	0.605	45	0.756	27	−20
					Total	0.5	**Total**	−1.5	−1.0

Recombination rate was estimated in 10-, 25- and 50-Mb sliding windows across the genome. Windows with significantly divergent recombination between Gough Island lines were identified by permutation. Tables above show significant regions constructed from overlapping windows for each window size and their per cent difference from the mean rate. The recombination rate in these genomic regions as measured in the heterogeneous stock (HS) is also shown for comparison. Total percentages are calculated from sums across intervals for a given window size.

Table 3 Correlation of recombination rates between Gough Island lines and heterogeneous stock (HS)

	50-Mb windows		25-Mb windows		10-Mb windows	
Correlation between	ρ	95% CI	ρ	95% CI	ρ	95% CI
Line A and Line B	0.909	0.905–0.914	0.913	0.909–0.916	0.882	0.877–0.886
Line A and HS	0.897	0.893–0.901	0.855	0.850–0.860	0.764	0.755–0.772
Line B and HS	0.925	0.922–0.927	0.891	0.887–0.895	0.798	0.791–0.805

Pearson correlation coefficients calculated for corresponding 10-, 25- and 50-Mb sliding windows across the genome with respective 95% confidence intervals. Correlation coefficients were highly significant for all comparisons.

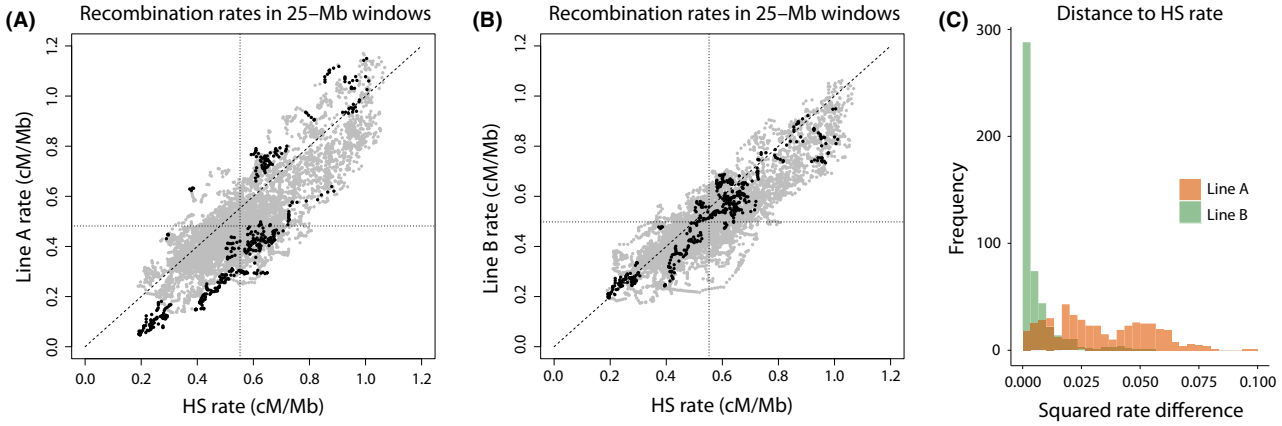

Fig. 3 Comparisons of recombination rates in Gough Island lines and the heterogeneous stock (HS). A comparison of recombination rates using 25-Mb sliding windows in (A) the HS mice and Gough Line A, and (B) the HS mice and Gough Line B. Each point represents a single 25-Mb window with respective recombination rates along the *x*-axis and *y*-axis. Windows that were significantly different between Gough Island Line A and Line B are highlighted in bold on these plots. (C) Squared difference in recombination rate between each Gough Island line and HS for these significantly different windows, showing substantially more dispersion from HS in Line A. [Colour figure can be viewed at wileyonlinelibrary.com].

(Fullerton *et al.* 2001; Rizzon *et al.* 2002; Jensen-Seaman *et al.* 2004; Freudenberg *et al.* 2009; Paigen *et al.* 2008; Paape *et al.* 2012; Farré *et al.* 2013; Kawakami *et al.* 2014; Liu *et al.* 2014). We examined whether these genomic features were also associated with recombination rate differences among individuals, *that is* between the two lines of GI mice. We estimated recombination rates in nonoverlapping windows of 10 Mb, 25 Mb and 50 Mb in the two GI lines and calculated the difference ($Rate_{LineA}$–$Rate_{LineB}$) between corresponding windows. Among the genomic features we evaluated, only the number of long terminal repeats (LTRs) was significantly correlated ($P < 0.05$) with the difference in recombination rate among GI lines at all three scales (Table 4). At the intermediate 25-Mb scale, we also detected a significant correlation between gene density and recombination rate difference. Structural rearrangements are one of the genomic features highly correlated with recombination rate variation that is absent from this analysis. The difficulty in detecting small rearrangements means that we cannot rule out the role they may be playing in recombination rate polymorphism among GI lines.

To determine whether regions of high or low recombination are enriched for recombination rate divergence, we computed correlations between the relative recombination rate differences among GI lines, $|Rate_{LineA}–Rate_{LineB}|$/Mean Rate, and recombination rate in HS mice (in nonoverlapping windows). We observed a significant negative correlation ($P < 0.05$) at the 10- and 50-Mb scale (Table 4), corresponding to higher relative variation in recombination rates in regions that experience less recombination.

PRDM9 and motifs

A portion of the kilobase-scale variation in recombination rate observed in mice is explained by specific sequence motifs (Winckler *et al.* 2005; Myers *et al.* 2008; Steiner *et al.* 2009). One of the best-studied motifs is the

Table 4 Correlation with variation in recombination rate between Gough Island lines

	50-Mb windows		25-Mb windows		10-Mb windows	
Genomic feature	ρ	*P*-value	ρ	*P*-value	ρ	*P*-value
GC content	0.019	0.82	−0.049	0.49	−0.053	0.44
CpG Islands	−0.116	0.53	−0.055	0.63	−0.100	0.14
Gene density	−0.010	0.90	−0.168	0.02	−0.112	0.10
Chromatin state	—	0.11	—	0.99	—	0.99
LINE	0.046	0.57	0.094	0.18	0.068	0.32
LTR	−0.222	< 0.01	−0.172	0.01	−0.141	0.04
Satellite	−0.041	0.62	0.000	0.99	0.000	0.99
Breakpoint regions	0.014	0.94	−0.046	0.68	−0.096	0.16
Distance to centromere	0.037	0.64	0.084	0.23	0.032	0.64
Recombination rate	−0.308	0.03	−0.142	0.15	−0.233	< 0.01

Correlation of recombination rate differences between Gough Island lines in 10-, 25- and 50-Mb nonoverlapping windows with selected genomic features. Pearson correlation coefficient and *P*-value presented for GC content, CpG islands, gene density, long interspersed elements (LINE), long terminal repeats (LTR) and satellite DNA from mouse reference annotations. For chromatin state, the most prevalent state in each window was used as a categorical variable and *P*-values reported are from an analysis of variance. Evolutionary breakpoint regions were identified by an analysis of synteny between human and mouse reference genomes using Cassis (see Methods). For correlation to recombination rate itself, absolute differences in rate between the Gough lines divided by their mean rate were compared to rates from the HS map.

13-bp consensus sequence bound by PRDM9, a H3K4 trimethyltransferase with a zinc finger DNA-binding domain (Hayashi *et al.* 2005) that regulates the location and intensity of recombination hotspots (Myers *et al.* 2010; Baudat *et al.* 2010; Parvanov *et al.* 2010). Variation in recombination at this fine scale depends on both allelic variation in PRDM9—found in different subspecies and strains of mice (Baudat *et al.* 2010; Kono *et al.* 2014; Smagulova *et al.* 2016)—and polymorphisms in or near DNA binding sites (Baker *et al.* 2015). We investigated whether these determinants of hotspot variation relate to recombination rate variation between GI lines. First, we found that the two GI lines do not harbour allelic differences in PRDM9 that have been previously associated with variation in recombination rate. Next, we tested another straightforward hypothesis: the difference in the number of predicted PRDM9 binding sites among GI lines is correlated with the difference in recombination rate across genomic intervals; Stevison *et al.* 2016 tested a similar hypothesis across different species. Using whole-genome sequences from the parents of both crosses, we counted predicted PRDM9 binding sites in intervals of divergent recombination and compared these values between the GI lines (see Methods). We found no evidence for an association of PRDM9 binding site number with either the direction or intensity of variation in recombination rate (Table S1, Supporting information). While we lack the resolution to detect among-line differences in recombination rate at the kb scale, our results argue against an important contribution of PRDM9 to differences at the ≥10-Mb scale.

Discussion

Our results reveal substantial polymorphism in the recombination rate within an isolated island population. Because the mice for this study were raised in a common environment, we interpret this polymorphism as being caused by genetic variation. Up to 28% of the genome is included within subchromosomal intervals that show divergent rates among Gough Island mice, and five chromosomes exhibit different map lengths. In contrast, the total genomewide rate does not significantly vary. Two hypotheses could explain this disparity among genomic scales. First, stabilizing selection could maintain a genomewide recombination rate even as variation accumulates at the subchromosomal level. This type of selection would mirror the molecular homeostasis that buffers against perturbations to the total crossover number in individual cells (Martini *et al.* 2006; Rosu *et al.* 2011; Cole *et al.* 2012; Lao *et al.* 2013). The meiotic requirement of at least one crossover per chromosome (or per chromosome arm) places a lower limit on the genomewide recombination rate. However, our discovery of polymorphism in the chromosomal recombination rate in the absence of significant differences for total number of crossovers suggests that factors beyond proper disjunction constrain the evolution of the genomewide rate. Indeed, experiments promoting an excess number of crossovers, with mutants that disable crossover-suppressing proteins, indicate a controlled upper bound that is independent of a biochemical maximum (Youds *et al.* 2010; De Muyt *et al.*

2012; Crismani *et al.* 2012). Other evidence for direct or indirect selection on overall crossover number includes the observation that mothers with higher genomewide recombination rates are more fecund (Kong *et al.* 2004; Stefansson *et al.* 2005; Fledel-Alon *et al.* 2009). Perhaps recombination rate at the subchromosomal level has little or no effect on fitness, thereby allowing polymorphism to accumulate. An alternative explanation for the disparity in variation among genomic scales is that selective constraints on recombination rate do not operate on the genomewide rate. If the lower limit, set by meiotic requirements, is truly dictated by karyotype, the focus of selection should fall on recombination rates at finer (chromosomal) scales. Under this scenario, evolutionary changes to recombination rate on finer scales since the common ancestor of the two GI lines have incidentally balanced such that the overall rate remains unchanged. In this model, the genomewide rate between these lines would presumably begin to diverge after more time passes.

We discovered that on the subchromosomal scale, recombination rate differences between GI lines and HS mice are asymmetric, with Line A showing more divergence. Perhaps this bias indicates a closer phylogenetic relationship between Line B and the HS mice. This seems unlikely given the history of the HS as an amalgam of classical inbred strains and the geographically singular origin of the GI mice. Alternatively, this bias might reflect the random sampling of recombination polymorphism from the GI population. Perhaps a small number of mutations modifying recombination rate are segregating in the population. Further genetic studies will be required to test this hypothesis.

Our identification of genomic correlates of recombination rate polymorphism provides additional clues into the dynamics of recombination rate evolution. Relative differences in recombination rate between GI lines were negatively correlated with the rate in the HS mice. This suggests that recombinationally cold regions are more likely to experience greater relative changes in recombination rate. We also found LTR density to be negatively correlated with differences in recombination rate between GI lines, suggesting that the evolution of recombination rate may be slower in these regions. LTR density has been strongly associated with regions of lower recombination in other organisms (Rizzon *et al.* 2002; Groenen *et al.* 2009), and LTR retrotransposons have been shown to influence double-strand break formation in meiosis (Sasaki *et al.* 2013).

A similar study of recombination rate variation in house mice (Dumont *et al.* 2011) provides an unusual opportunity to compare the evolution of recombination rate on two timescales. Dumont *et al.* (2011) statistically compared genetic maps from representatives of two house mouse subspecies, *M. m. musculus* and *M. m. castaneus*. Like us, these authors constructed genetic maps from F_2 intercrosses to the WSB/EiJ reference strain, using sample sizes (580 and 554 F_2s in the two crosses) similar to ours. Thirty-one divergent windows were detected, differing on average by 4.5 cM between the *M. m. musculus* and *M. m. castaneus* maps. Divergent windows between the two GI lines are fewer and show smaller differences in recombination rate, consistent with the more recent divergence of these lines compared with *M. m. musculus* and *M. m. castaneus*. Eight of the divergent intervals we identified overlap with genomic windows that significantly differ between strains of *M. m. musculus* and *M. m. castaneus*. This is approximately consistent with the amount of overlap expected by chance given the size of the divergent intervals. However, the absence of divergent intervals on the X chromosome in the GI lines is notable given their disproportionate localization to this chromosome in the intersubspecific comparison. Our experimental design has reduced power to detect differences on the X chromosome, as the X does not recombine in F_1 males, but this is an issue shared with the previous study.

We temper our conclusions about recombination rate evolution by noting a few challenges with our experimental design. First, F_2 genetic maps reveal average recombination rates in F_1 females and F_1 males. In mice, sex is a key determinant of recombination rate on multiple genomic scales (Lynn *et al.* 2005; Paigen *et al.* 2008; Cox *et al.* 2009; Liu *et al.* 2014), raising the prospect that females and males could differ in patterns of polymorphism. Our study is blind to this axis of variation. Second, although we detected differences among GI lines on the Mb scale, many more meioses would be required to find variation on the scale of recombination hotspots. A parallel issue is our inability to detect minor structural changes in the mouse genome. Some differences in mapping distance between GI lines could reflect inversions and other structural rearrangements segregating within the GI population. Third, the statistical power to detect differences in recombination rate depends on the total number of crossovers observed. Contrasting patterns across chromosomes, like the absence of differences at finer scales on some chromosomes, may be due to these differences in power. Finally, our interpretation of genetic map differences as polymorphism among GI lines assumes that crossing to the common reference strain (WSB/EiJ) had similar effects on recombination for both lines. Although there is no obvious reason to question this assumption, it is important to remember that the recombination we profiled occurred in F_1s and not in the GI lines. Immunocytology suggests that the genomewide recombination

rate is higher in GI mice than in WSB/EiJ (Dumont & Payseur 2011a).

The observation of substantial differences in recombination rate among a few mice drawn from an isolated population suggests that genetic variation in recombination rate is likely to be pervasive among wild house mice. The balance of evolutionary factors that govern recombination rate in nature remains unclear. A coherent model for the evolution of recombination rate will need to integrate and explain patterns of variation found on each genomic scale.

Acknowledgements

This research was supported by a National Institutes of Health (NIH) grant, R01 GM100426A, to BAP. Participation by RJW was supported by a National Institute of General Medical Sciences training grant to the University of Wisconsin (UW), and a National Library of Medicine training grant to UW in Computation and Informatics in Biology and Medicine, NLM 5T15LM007359.

References

Anderson LK, Reeves A, Webb LM, Ashley T (1999) Distribution of crossing over on mouse synaptonemal complexes using immunofluorescent localization of MLH1 protein. *Genetics*, **151**, 1569–1579.

Backstrom N, Forstmeier W, Schielzeth H *et al.* (2010) The recombination landscape of the zebra finch *Taeniopygia guttata* genome. *Genome Research*, **20**, 485–495.

Baier B, Hunt P, Broman KW, Hassold T (2014) Variation in genome-wide levels of meiotic recombination is established at the onset of prophase in mammalian males. *Plos Genetics*, **10**, e1004125.

Baker CL, Kajita S, Walker M *et al.* (2015) PRDM9 drives evolutionary erosion of hotspots in *Mus musculus* through haplotype-specific initiation of meiotic recombination. *Plos Genetics*, **11**, e1004916.

Baudat F, Buard J, Grey C *et al.* (2010) PRDM9 Is a major determinant of meiotic recombination hotspots in humans and mice. *Science*, **327**, 836–840.

Baudet C, Lemaitre C, Dias Z, Gautier C, Tannier E, Sagot MF (2010) Cassis: detection of genomic rearrangement breakpoints. *Bioinformatics*, **26**, 1897–1898.

Beadle GW (1932) A possible influence of the spindle fibre on crossing-over in *Drosophila*. *Proceedings of the National Academy of Sciences of the United States of America*, **18**, 160–165.

Begun D, Aquadro C (1992) Levels of naturally-occurring DNA polymorphism correlate with recombination rates in *D. melanogaster*. *Nature*, **356**, 519–520.

Bolcun-Filas E, Schimenti JC (2012) Genetics of Meiosis and Recombination in Mice. In: *International Review of Cell and Molecular Biology*, vol. **298**(ed Jeon K. W.), pp. 179–227. Elsevier Academic Press Inc, San Diego.

Bomblies K, Higgins JD, Yant L (2015) Meiosis evolves: adaptation to external and internal environments. *New Phytologist*, **208**, 306–323.

Brick K, Smagulova F, Khil P, Camerini-Otero RD, Petukhova GV (2012) Genetic recombination is directed away from functional genomic elements in mice. *Nature*, **485**, 642–645.

Broman KW, Sen S (2009) *A Guide to QTL Mapping with R/qtl*. Springer, New York.

Broman KW, Murray JC, Sheffield VC, White RL, Weber JL (1998) Comprehensive human genetic maps: individual and sex-specific variation in recombination. *American Journal of Human Genetics*, **63**, 861–869.

Brunschwig H, Levi L, Ben-David E, Williams RW, Yakir B, Shifman S (2012) Fine-scale maps of recombination rates and hotspots in the mouse genome. *Genetics*, **191**, 757–764.

Buard J, Rivals E, de Segonzac DD *et al.* (2014) Diversity of Prdm9 zinc finger array in wild mice unravels new facets of the evolutionary turnover of this coding minisatellite. *PLoS ONE*, **9**, e85021.

Burt DW (2002) Origin and evolution of avian microchromosomes. *Cytogenetic and Genome Research*, **96**, 97–112.

Carter TC, Falconer DS (1951) Stocks for detecting linkage in the mouse, and the theory of their design. *Jour Genetics*, **50**, 307–323.

Charlesworth B, Charlesworth D (1985) Genetic-variation in recombination in Drosophila. 1. Responses to selection and preliminary genetic-analysis. *Heredity*, **54**, 71–83.

Chinnici J (1971) Modification of recombination frequency in Drosophila. 1. Selection for increased and decreased crossing over. *Genetics*, **69**, 71–83.

Cole F, Kauppi L, Lange J *et al.* (2012) Homeostatic control of recombination is implemented progressively in mouse meiosis. *Nature Cell Biology*, **14**, 424–430.

Cole F, Baudat F, Grey C, Keeney S, de Massy B, Jasin M (2014) Mouse tetrad analysis provides insights into recombination mechanisms and hotspot evolutionary dynamics. *Nature Genetics*, **46**, 1072–1080.

Comeron JM, Ratnappan R, Bailin S (2012) The many landscapes of recombination in *Drosophila melanogaster*. *Plos Genetics*, **8**, e1002905.

Coop G, Wen X, Ober C, Pritchard JK, Przeworski M (2008) High-resolution mapping of crossovers reveals extensive variation in fine-scale recombination patterns among humans. *Science*, **319**, 1395–1398.

Cox A, Ackert-Bicknell CL, Dumont BL *et al.* (2009) A new standard genetic map for the laboratory mouse. *Genetics*, **182**, 1335–1344.

Crismani W, Girard C, Froger N *et al.* (2012) FANCM Limits Meiotic Crossovers. Science, **336**, 1588–1590.

Cullen M, Perfetto SP, Klitz W, Nelson G, Carrington M (2002) High-resolution patterns of meiotic recombination across the human major histocompatibility complex. *American Journal of Human Genetics*, **71**, 759–776.

De Muyt A, Jessop L, Kolar E *et al.* (2012) BLM Helicase Ortholog Sgs1 is a central regulator of meiotic recombination intermediate metabolism. *Molecular Cell*, **46**, 43–53.

Dumont BL, Payseur BA (2008) Evolution of the genomic rate of recombination in mammals. *Evolution*, **62**, 276–294.

Dumont BL, Payseur BA (2011a) Evolution of the genomic recombination rate in murid rodents. *Genetics*, **187**, 643–657.

Dumont BL, Payseur BA (2011b) Genetic analysis of genome-scale recombination rate evolution in house mice. *Plos Genetics*, **7**, e1002116.

Dumont BL, White MA, Steffy B, Wiltshire T, Payseur BA (2011) Extensive recombination rate variation in the house mouse species complex inferred from genetic linkage maps. *Genome Research*, **21**, 114–125.

Ernst J, Kellis M (2012) CHROMHMM: automating chromatin-state discovery and characterization. *Nature Methods*, **9**, 215–216.

Evans DM, Cardon LR (2005) A comparison of linkage disequilibrium patterns and estimated population recombination rates across multiple populations. *American Journal of Human Genetics*, **76**, 681–687.

Eyre-Walker A (1993) Recombination and mammalian genome evolution. *Proceedings of the Royal Society B-Biological Sciences*, **252**, 237–243.

Farré M, Micheletti D, Ruiz-Herrera A (2013) Recombination rates and genomic shuffling in human and chimpanzee—a new twist in the chromosomal speciation theory. *Molecular Biology and Evolution*, **30**, 853–864.

Felsenstein J (1974) The evolutionary advantage of recombination. *Genetics*, **78**, 737–756.

Fledel-Alon A, Wilson DJ, Broman K *et al.* (2009) Broad-scale recombination patterns underlying proper disjunction in humans. *Plos Genetics*, **5**, e1000658.

Fledel-Alon A, Leffler EM, Guan Y, Stephens M, Coop G, Przeworski M (2011) Variation in human recombination rates and its genetic determinants. *PLoS ONE*, **6**, e20321.

Freudenberg J, Wang M, Yang Y, Li W (2009) Partial correlation analysis indicates causal relationships between GC-content, exon density and recombination rate in the human genome. *BMC Bioinformatics*, **10**, S66.

Froehlich J, Vozdova M, Kubickova S, Cernohorska H, Sebestova H, Rubes J (2015) Variation of meiotic recombination rates and MLH1 foci distribution in spermatocytes of cattle, sheep and goats. *Cytogenetic and Genome Research*, **146**, 211–221.

Fullerton SM, Carvalho AB, Clark AG (2001) Local rates of recombination are positively correlated with GC content in the human genome. *Molecular Biology and Evolution*, **18**, 1139–1142.

Gerton JL, DeRisi J, Shroff R, Lichten M, Brown PO, Petes TD (2000) Global mapping of meiotic recombination hotspots and coldspots in the yeast *Saccharomyces cerevisiae*. *Proceedings of the National Academy of Sciences of the United States of America*, **97**, 11383–11390.

Giraut L, Falque M, Drouaud J, Pereira L, Martin OC, Mézard C (2011) Genome-wide crossover distribution in arabidopsis thaliana meiosis reveals sex-specific patterns along chromosomes. *PLoS Genetics*, **7**, e1002354.

Graffelman J, Balding DJ, Gonzalez-Neira A, Bertranpetit J (2007) Variation in estimated recombination rates across human populations. *Human Genetics*, **122**, 301–310.

Grant CE, Bailey TL, Noble WS (2011) FIMO: scanning for occurrences of a given motif. *Bioinformatics*, **27**, 1017–1018.

Gray MM, Wegmann D, Haasl RJ *et al.* (2014) Demographic history of a recent invasion of house mice on the isolated Island of Gough. *Molecular Ecology*, **23**, 1923–1939.

Gray MM, Parmenter MD, Hogan CA *et al.* (2015) Genetics of rapid and extreme size evolution in island mice. *Genetics*, **201**, 213–228.

Grey C, Barthès P, Friec GC-L, Langa F, Baudat F, de Massy B (2011) Mouse PRDM9 DNA-binding specificity determines sites of histone H3 lysine 4 trimethylation for initiation of meiotic recombination. *PLoS Biology*, **9**, e1001176.

Griffiths RC, Marjoram P (1996) Ancestral inference from samples of DNA sequences with recombination. *Journal of Computational Biology*, **3**, 479–502.

Groenen MAM, Wahlberg P, Foglio M *et al.* (2009) A high-density SNP-based linkage map of the chicken genome reveals sequence features correlated with recombination rate. *Genome Research*, **19**, 510–519.

Hassold T, Hall H, Hunt P (2007) The origin of human aneuploidy: where we have been, where we are going. *Human Molecular Genetics*, **16**, R203–R208.

Hayashi K, Yoshida K, Matsui Y (2005) A histone H3 methyltransferase controls epigenetic events required for meiotic prophase. *Nature*, **438**, 374–378.

Holloway JK, Booth J, Edelmann W, McGowan CH, Cohen PE (2008) MUS81 generates a subset of MLH1-MLH3-independent crossovers in mammalian meiosis. *Plos Genetics*, **4**, e1000186.

Hunter CM, Huang W, Mackay TFC, Singh ND (2016) The genetic architecture of natural variation in recombination rate in *Drosophila melanogaster*. *Plos Genetics*, **12**, e1005951.

Jeffreys AJ, Kauppi L, Neumann R (2001) Intensely punctate meiotic recombination in the class II region of the major histocompatibility complex. *Nature Genetics*, **29**, 217–222.

Jensen-Seaman MI, Furey TS, Payseur BA *et al.* (2004) Comparative recombination rates in the rat, mouse, and human genomes. *Genome Research*, **14**, 528–538.

Johnston SE, Berenos C, Slate J, Pemberton JM (2016) Conserved genetic architecture underlying individual recombination rate variation in a wild population of soay sheep (*Ovis aries*). *Genetics*, **203**, 583–598.

Kawakami T, Smeds L, Backstrom N *et al.* (2014) A high-density linkage map enables a second-generation collared flycatcher genome assembly and reveals the patterns of avian recombination rate variation and chromosomal evolution. *Molecular Ecology*, **23**, 4035–4058.

Kidwell M, Kidwell J (1976) Selection for male recombination in *Drosophila melanogaster*. *Genetics*, **84**, 333–351.

Kochakpour N, Moens PB (2008) Sex-specific crossover patterns in Zebrafish (*Danio rerio*). *Heredity*, **100**, 489–495.

Koehler KE, Cherry JP, Lynn A, Hunt PA, Hassold TJ (2002) Genetic control of mammalian meiotic recombination. I. Variation in exchange frequencies among males from inbred mouse strains. *Genetics*, **162**, 297–306.

Kong A, Gudbjartsson DF, Sainz J *et al.* (2002) A high-resolution recombination map of the human genome. *Nature Genetics*, **31**, 241–247.

Kong A, Barnard J, Gudbjartsson DF *et al.* (2004) Recombination rate and reproductive success in humans. *Nature Genetics*, **36**, 1203–1206.

Kong A, Thorleifsson G, Stefansson H *et al.* (2008) Sequence variants in the RNF212 gene associate with genome-wide recombination rate. *Science*, **319**, 1398–1401.

Kono H, Tamura M, Osada N *et al.* (2014) PRDM9 polymorphism unveils mouse evolutionary tracks. *DNA Research*, **21**, 315–326.

Lander E, Green P (1987) Construction of multilocus genetic-linkage maps in humans. *Proceedings of the National Academy of Sciences of the United States of America*, **84**, 2363–2367.

Lao JP, Cloud V, Huang C-C *et al.* (2013) Meiotic crossover control by concerted action of Rad51-Dmc1 in homolog template bias and robust homeostatic regulation. *Plos Genetics*, **9**, e1003978.

Leek JT, Storey JD (2011) The joint null criterion for multiple hypothesis tests. *Statistical Applications in Genetics and Molecular Biology*, **10**, 28.

Lemaitre C, Tannier E, Gautier C, Sagot M-F (2008) Precise detection of rearrangement breakpoints in mammalian chromosomes. *BMC Bioinformatics*, **9**, 286.

Li H, Durbin R (2009) Fast and accurate short read alignment with Burrows-Wheeler transform. *Bioinformatics*, **25**, 1754–1760.

Li H, Handsaker B, Wysoker A *et al.* (2009) The sequence alignment/map format and SAMtools. *Bioinformatics*, **25**, 2078–2079.

Liu EY, Morgan AP, Chesler EJ, Wang W, Churchill GA, de Villena FP (2014) High-resolution sex-specific linkage maps of the mouse reveal polarized distribution of crossovers in male germline. *Genetics*, **197**, 91–106.

Lynn A, Ashley T, Hassold T (2004) Variation in human meiotic recombination. *Annual Review of Genomics and Human Genetics*, **5**, 317–349.

Lynn A, Schrump S, Cherry J, Hassold T, Hunt P (2005) Sex, not genotype, determines recombination levels in mice. *American Journal of Human Genetics*, **77**, 670–675.

Ma L, O'Connell JR, VanRaden PM *et al.* (2015) Cattle sex-specific recombination and genetic control from a large pedigree analysis. *Plos Genetics*, **11**, e1005387.

Mahtani MM, Willard HF (1998) Physical and genetic mapping of the human X chromosome centromere: repression of recombination. *Genome Research*, **8**, 100–110.

Martini E, Diaz RL, Hunter N, Keeney S (2006) Crossover homeostasis in yeast meiosis. *Cell*, **126**, 285–295.

de Massy B (2013) Initiation of Meiotic Recombination: How and Where? Conservation and Specificities Among Eukaryotes. In: *Annual Review of Genetics*, vol. **47** (eds Bassler B. L., Lichten M., Schupbach G.), pp. 563–599. Palo Alto, Annual Reviews.

Mather K (1936) The determination of position in crossing-over. *Journal of Genetics*, **33**, 207–235.

McVean GAT, Myers SR, Hunt S, Deloukas P, Bentley DR, Donnelly P (2004) The fine-scale structure of recombination rate variation in the human genome. *Science*, **304**, 581–584.

Morgan AP, Fu C-P, Kao C-Y *et al.* (2016) The mouse universal genotyping array: from substrains to subspecies. *G3-Genes Genomes, Genetics*, **6**, 263–279.

Mouse ENCODE Consortium, Stamatoyannopoulos JA, Snyder M *et al.* (2012) An encyclopedia of mouse DNA elements (Mouse ENCODE). *Genome Biology*, **13**, 418.

Murdoch B, Owen N, Shirley S, Crumb S, Broman KW, Hassold T (2010) Multiple loci contribute to genome-wide recombination levels in male mice. *Mammalian Genome*, **21**, 550–555.

Myers S, Freeman C, Auton A, Donnelly P, McVean G (2008) A common sequence motif associated with recombination hot spots and genome instability in humans. *Nature Genetics*, **40**, 1124–1129.

Myers S, Bowden R, Tumian A *et al.* (2010) Drive against hotspot motifs in primates implicates the PRDM9 gene in meiotic recombination. *Science*, **327**, 876–879.

Neumann R, Jeffreys AJ (2006) Polymorphism in the activity of human crossover hotspots independent of local DNA sequence variation. *Human Molecular Genetics*, **15**, 1401–1411.

Otto SP, Lenormand T (2002) Resolving the paradox of sex and recombination. *Nature Reviews Genetics*, **3**, 252–261.

Paape T, Zhou P, Branca A, Briskine R, Young N, Tiffin P (2012) Fine-scale population recombination rates, hotspots, and correlates of recombination in the *Medicago truncatula* genome. *Genome Biology and Evolution*, **4**, 726–737.

Paigen K, Petkov P (2010) Mammalian recombination hot spots: properties, control and evolution. *Nature Reviews Genetics*, **11**, 221–233.

Paigen K, Szatkiewicz JP, Sawyer K *et al.* (2008) The recombinational anatomy of a mouse chromosome. *Plos Genetics*, **4**, e1000119.

Parvanov ED, Petkov PM, Paigen K (2010) PRDM9 controls activation of mammalian recombination hotspots. *Science*, **327**, 835.

Poissant J, Hogg JT, Davis CS, Miller JM, Maddox JF, Coltman DW (2010) Genetic linkage map of a wild genome: genomic structure, recombination and sexual dimorphism in bighorn sheep. *BMC Genomics*, **11**, 524.

Ptak SE, Hinds DA, Koehler K *et al.* (2005) Fine-scale recombination patterns differ between chimpanzees and humans. *Nature Genetics*, **37**, 429–434.

Rizzon C, Marais G, Gouy M, Biemont C (2002) Recombination rate and the distribution of transposable elements in the *Drosophila melanogaster* genome. *Genome Research*, **12**, 400–407.

Rockman MV, Kruglyak L (2009) Recombinational landscape and population genomics of *Caenorhabditis elegans*. *Plos Genetics*, **5**, e1000419.

Ross CR, DeFelice DS, Hunt GJ, Ihle KE, Amdam GV, Rueppell O (2015) Genomic correlates of recombination rate and its variability across eight recombination maps in the western honey bee (*Apis mellifera* L.). *BMC Genomics*, **16**, 107.

Rosu S, Libuda DE, Villeneuve AM (2011) Robust crossover assurance and regulated interhomolog access maintain meiotic crossover number. *Science*, **334**, 1286–1289.

Sandor C, Li W, Coppieters W, Druet T, Charlier C, Georges M (2012) Genetic variants in REC8, RNF212, and PRDM9 influence male recombination in cattle. *Plos Genetics*, **8**, e1002854.

Sasaki M, Tischfield SE, van Overbeek M, Keeney S (2013) Meiotic recombination initiation in and around retrotransposable elements in *Saccharomyces cerevisiae*. *Plos Genetics*, **9**, e1003732.

Schierup MH, Hein J (2000) Consequences of recombination on traditional phylogenetic analysis. *Genetics*, **156**, 879–891.

Segura J, Ferretti L, Ramos-Onsins S *et al.* (2013) Evolution of recombination in eutherian mammals: insights into mechanisms that affect recombination rates and crossover interference. *Proceedings of the Royal Society B-Biological Sciences*, **280**. UNSP 20131945.

Shifman S, Bell JT, Copley RR *et al.* (2006) A high-resolution single nucleotide polymorphism genetic map of the mouse genome. *Plos Biology*, **4**, 2227–2237.

Singhal S, Leffler EM, Sannareddy K *et al.* (2015) Stable recombination hotspots in birds. *Science*, **350**, 928–932.

Smagulova F, Brick K, Pu Y, Camerini-Otero RD, Petukhova GV (2016) The evolutionary turnover of recombination hot spots contributes to speciation in mice. *Genes & Development*, **30**, 266–280.

Smeds L, Mugal CF, Qvarnström A, Ellegren H (2016) High-resolution mapping of crossover and non-crossover

recombination events by whole-genome re-sequencing of an avian pedigree. *PLoS Genetics*, **12**, e1006044.
Smukowski CS, Noor MAF (2011) Recombination rate variation in closely related species. *Heredity*, **107**, 496–508.
Stefansson H, Helgason A, Thorleifsson G *et al.* (2005) A common inversion under selection in Europeans. *Nature Genetics*, **37**, 129–137.
Steiner WW, Steiner EM, Girvin AR, Plewik LE (2009) Novel nucleotide sequence motifs that produce hotspots of meiotic recombination in *Schizosaccharomyces pombe*. *Genetics*, **182**, 459–469.
Stevison LS, Woerner AE, Kidd JM *et al.* (2016) The time scale of recombination rate evolution in great apes. *Molecular Biology and Evolution*, **33**, 928–945.
Storey JD, Tibshirani R (2003) Statistical significance for genomewide studies. *Proceedings of the National Academy of Sciences of the United States of America*, **100**, 9440–9445.
Talbert PB, Henikoff S (2010) Centromeres convert but don't cross. *Plos Biology*, **8**, e1000326.
Tiemann-Boege I, Calabrese P, Cochran DM, Sokol R, Arnheim N (2006) High-resolution recombination patterns in a region of human chromosome. *Plos Genetics*, **2**, 682–692.
True JR, Mercer JM, Laurie CC (1996) Differences in crossover frequency and distribution among three sibling species of *Drosophila*. *Genetics*, **142**, 507–523.
Tsubouchi H, Roeder GS (2003) The importance of genetic recombination for fidelity of chromosome pairing in meiosis. *Developmental Cell*, **5**, 915–925.
Ullastres A, Farré M, Capilla L, Ruiz-Herrera A (2014) Unraveling the effect of genomic structural changes in the rhesus macaque—implications for the adaptive role of inversions. *BMC Genomics*, **15**, 530.
de Villena FP-M, Sapienza C (2001) Recombination is proportional to the number of chromosome arms in mammals. *Mammalian Genome*, **12**, 318–322.
Webb AJ, Berg IL, Jeffreys A (2008) Sperm cross-over activity in regions of the human genome showing extreme breakdown of marker association. *Proceedings of the National Academy of Sciences of the United States of America*, **105**, 10471–10476.
Winckler W, Myers SR, Richter DJ *et al.* (2005) Comparison of fine-scale recombination rates in humans and chimpanzees. *Science*, **308**, 107–111.
Youds JL, Mets DG, McIlwraith MJ *et al.* (2010) RTEL-1 enforces meiotic crossover interference and homeostasis. *Science*, **327**, 1254–1258.
Yue F, Cheng Y, Breschi A et al. (2014) A comparative encyclopedia of DNA elements in the mouse genome. *Nature*, **515**, 355–364.

RJW and BAP designed the study. MMG and MDP performed crosses and collected data. RJW and KWB conducted analyses. RJW and BAP wrote the manuscript.

Data accessibility

The genotypes of mice used in this study are available from the QTL Archive at the Jackson Laboratory, http://phenome.jax.org/db/q?rtn=projects/projdet&reqprojid=539. Sequences of the four parental GI mice are available under NCBI Bioproject Accession: PRJNA352398.

Supporting information

Additional supporting information may be found in the online version of this article.

Table S1 Regions of divergent recombination and their predicted PRDM9 binding sites.

Table S2 Marker density and number of crossovers by chromosome.